

# Various Approaches for Solving Problems in Heat Conduction with Phase Change

Mohamad MUHIEDDINE<sup>†\*</sup>

<sup>†</sup>*IRISA, Campus de Beaulieu*

<sup>\*</sup>*Archéosciences, UMR 6566*

*35042 Rennes, France*

mohamad.muhieddine@irisa.fr

Édouard CANOT<sup>†</sup>

<sup>†</sup>*IRISA, Campus de Beaulieu*

*35042 Rennes, France*

edouard.canot@irisa.fr

Ramiro MARCH<sup>\*</sup>

<sup>\*</sup>*Archéosciences, UMR 6566*

*35042 Rennes, France*

ramiro.march@univ-rennes1.fr

## Abstract

---

This paper treats a one dimensional phase-change problem, 'ice melting', by a vertex-centered finite volume method. Numerical solutions are obtained by using two approaches where the first one is based on the heat conduction equation with the basic grid (improved by introducing a new adaptive mesh technique), latent heat source approach (LHA), while the second uses the equivalent thermodynamic parameters defined by considering the apparent heat capacity method (AHC). A comparison between the two approaches is presented, furthermore the accuracy and flexibility of the numerical methods are verified by comparing the results with existing analytical solutions. Results indicate that phase-change problems can be handled easily with excellent accuracies by using the AHC method.

**Key words** : Phase-change, computational fluid dynamics, latent heat, finite volumes, rolling mesh, self-adaptive mesh, apparent capacity method, moving boundary problem.

---

## Nomenclature

$C_p$	:	Specific heat,
$E$	:	Energy,
$H$	:	Total enthalpy,
$T$	:	Temperature,
$k$	:	Thermal conductivity,
$L$	:	Latent heat of fusion,
$U$	:	Step function,
$V$	:	Control volume,
$Q$	:	Accumulation latent heat,
$Q^{total}$	:	Total latent heat,
$\Delta x$	:	Control volume size,
$\Delta\phi$	:	Heat flux difference,
$\Delta t$	:	Time step,
$\Delta T$	:	Temperature semi-interval,
$\alpha$	:	Weighting factor,
$\theta$	:	Solid fraction,
$\rho$	:	Density,
$\phi$	:	Volumetric fraction,
$\xi$	:	Interface position,
$\delta$	:	Dirac delta function.
Subscripts		
0	:	Initial phase,
$f$	:	Phase changing point,
$i$	:	node index,
$l$	:	Liquid phase,
$s$	:	Solid phase.

## 1 Introduction

Melting processes are classified as moving boundary problems which have been of special interest due to the inherent difficulties associated with the non-linearity of the interface conditions and the unknown locations of the moving boundaries. This paper is concerned with a numerical method for solving a one dimensional phase-change problem leading to further studies on energy-saving and quality improvements. Solving such problem of phase change, where analytical solution exists, enables us to choose the best approach to solve our problem of interest “the forced evaporation in saturated porous media” which has a direct application in the study of prehistoric fire.

Over the years, a number of related computational works have employed various techniques in the analysis of phase change problems. Several important theoretical results on the existence, the uniqueness and the properties of classical solutions are available in the literature [MUE 65], [CAN 67], [LUI 68], [BEJ 03]. Besides, most analytical solutions deal with for 1-D geometries with very particular boundary conditions hence, cannot be generalize to multidimensional problems. Thus, many

numerical schemes [VOL 87], [KIM 90], [WAN 00], [SAV 03], [JAV 06], have been proposed to study transient heat conduction problems with phase change in one, two and three dimensions, but two formulations are predominant in the numerical analysis. The first one is referred to as the 'front-tracking method' in which the position of the moving front is determined at each time step [ASK 87], and must always correspond to a node or edges mesh. The use of this numerical method can usually eliminate the oscillations obtained by using the fixed grid method, and allows for more precise solutions. However, it is poorly suited to multi-dimensional problems due to the algorithm's difficult implementation and the large computational cost.

The second formulation, based on the use of the heat enthalpy concept [BON 73], [PRA 04], recasts the problem in such a way that the conditions on the moving phase front are absorbed into new equations, and the problem is solved without explicit reference to the position of the internal boundary (interface position). Its position is determined a posteriori, when the solution is complete. The major problem with the latter method is that it is not very accurate. In addition, this formulation often requires the use of algorithms to correct the solution in order not to miss the absorption or the release of latent heat.

Other publications related to heat conduction problems with phase change, using either finite difference or finite element method or both, can be found in references [PAW 85], [GRA 89], [SAV 03]. All of them are of interest, but the most interesting numerical method in our case is based on the finite volume formulation which has the important feature that the resulting solution ensures that the conservation of quantities involved such as mass, momentum and energy is exactly satisfied not only over any group of control volumes but over the whole domain of computation, which is not the reality when dealing with finite difference methods. Finite element approach [GUI 74] takes advantage in the ability to divide the domain of interest in elementary subdomains, namely elements. It may therefore handle problems with steep gradients and may deal with irregular geometric configurations. Comparing finite element method with finite volume one, this last still more conservative and so more adequate to solve our problem.

This work chooses to use two approaches, the latent heat accumulation approach (LHA) [PRA 04] and the apparent heat capacity method (AHC) [BON 73]. The numerical methods based on enthalpy formulation of the problem have been studied in [BON 73], [CIV 87], [LAM 04], [PRA 04], [MUH 08]. However, the algorithm proposed for the LHA method is rather similar to that of Prapainop [PRA 04], where the enthalpy formulation has been used to construct an approximation scheme. The finite volume method is implemented over a special rolling mesh in the LHA composed of a basic regular grid which is recursively refined near the interface. In the AHC a fixed grid scheme has been used.

## 2 Mathematical model for simulating problem with phase change

Only conduction is considered as a heat transfer mode. The physical properties which characterize the solid and liquid phase, such as specific heat and conductivity,

are constant for a given phase, it is likely not to be the case in reality but our model is able to take into account non-constant parameters. This proposed approximation supposes that all radiative effects within ice melting are neglected. In the following, we shortly describe equations for a melting problem, with the further approximation that density is the same for the two phases.

## 2.1 Equations and boundary conditions

Our melting problem is characterized by solving the partial differential equation obtained by combining Fourier's law of heat conduction and the law of conservation of energy which states that the rate of energy accumulation within a control volume of size  $\Delta x$  equals the net heat transfer by conduction

$$\frac{\partial}{\partial t} [\rho C_p T \Delta x] = \Delta \phi \quad (1)$$

where  $\Delta \phi$  is the heat flux difference at the boundaries of the control volume. The problem deals with a semi-infinite region of ice initially at  $T_0 = -10^\circ C$ . At time  $t > 0$ , the boundary at  $x = 0$  is suddenly kept at  $T_w = 20^\circ C$ . The governing equations for the temperature  $T(x, t)$  are formulated as follows :

$$\begin{cases} \rho C_l \frac{\partial T}{\partial t} = \frac{\partial}{\partial x} \left[ k_l \frac{\partial T}{\partial x} \right] & 0 < x < \xi(t), \quad t > 0 \\ T_l(0, t) = T_w & t > 0 \end{cases} \quad (2)$$

$$\begin{cases} \rho C_s \frac{\partial T}{\partial t} = \frac{\partial}{\partial x} \left[ k_s \frac{\partial T}{\partial x} \right] & \xi(t) < x < +\infty, \quad t > 0 \\ T_s(\infty, t) = T_0 & t > 0 \end{cases} \quad (3)$$

and for  $t = 0$

$$T(x, 0) = T_0 \quad \forall x \in [0, \infty[$$

where  $\rho = \rho_s = \rho_l$  is the density,  $C$  is the specific heat,  $\xi(t)$  is the interface position, and the subscripts  $s$  and  $l$  indicate the solid and liquid phases, respectively.

At the interface, the heat flux condition is written as [BON 73] :

$$k_l \frac{\partial T_l}{\partial x} - k_s \frac{\partial T_s}{\partial x} = -\rho L \frac{d\xi}{dt} \quad \text{at } x = \xi(t) \quad (4)$$

where  $L$  is the latent heat coefficient and  $d\xi/dt$  is the velocity of this interface. During the melting process, the liquid/solid front, which absorbs massive latent heat, continuously progresses through the medium. Moreover, the temperature verifies :

$$T_l = T_s = T_f \quad \text{at } x = \xi(t)$$

where  $T_f$  is the melting temperature.

At the initial time, the interface is assumed to be at position zero (*i.e.*,  $\xi(0) = 0$ ).

### 3 Analytical solution

Exact solutions of 1D phase change of a semi-infinite slab were analyzed by Carslaw and Jaeger [CAR 59] and KU and Chan [KU 90] with the moving front approach. The exact temperature distributions in solid,  $T_s$ , and in liquid,  $T_l$ , are respectively :

$$\begin{cases} T_l = T_w + (T_f - T_w) \frac{\operatorname{erf}(x^*)}{\operatorname{erf}(x_{sl}^*)} & \text{when } 0 < x^* < x_{sl}^* \\ T_s = T_0 + (T_f - T_0) \frac{\operatorname{erfc}(\sqrt{\mu_l/\mu_s}x^*)}{\operatorname{erfc}(\sqrt{\mu_l/\mu_s}x_{sl}^*)} & \text{when } x_{sl}^* < x^* < \infty \end{cases} \quad (5)$$

where  $x^* = x/2\sqrt{\mu_l t}$  is the dimensionless position and  $\mu = k/\rho C$  is the thermal diffusivity. The two values are calculated from corresponding mechanical properties for both solid  $\mu_s$  and liquid  $\mu_l$  values. The values of dimensionless position of solid-liquid interface  $x_{sl}^*$  are obtained via the nonlinear algebraic equation :

$$\frac{T_f - T_0}{T_f - T_w} \frac{k_s}{k_l} \sqrt{\frac{\mu_l}{\mu_s}} \frac{\exp(-(\mu_l/\mu_s)(x_{sl}^*)^2)}{\operatorname{erfc}(\sqrt{\mu_l/\mu_s}x_{sl}^*)} + \frac{\exp(-(x_{sl}^*)^2)}{\operatorname{erf}(x_{sl}^*)} - \frac{\sqrt{\pi}x_{sl}^*L}{C_l(T_f - T_w)} = 0 \quad (6)$$

### 4 Numerical method

The set of equations presented above are cast in the usual finite volume form for a finite domain (actually of length  $2m$ ), under a vertex centered formulation: each cell (or control volume) encloses exactly one data node at  $x_i$  and its boundaries are always computed as the center of two consecutive nodes, so that we obtain a good accuracy in the gradient estimation. We denote by  $T_i$  the whole approximate solution, the location of any variables being indicated by subscripts.

The time domain is divided into an arbitrary number of constant time steps of size  $\Delta t$ . Variables at time  $t$  are indicated by the superscript 0. In contrast, the variables at time level  $t + \Delta t$  are not superscripted.

For instance, the temperature at face  $i + \frac{1}{2}$  is  $T_{i+\frac{1}{2}} = T_i f_{i+\frac{1}{2}} + T_{i+1} (1 - f_{i+\frac{1}{2}})$  where  $f_{i+\frac{1}{2}} = (2\delta x_{i+\frac{1}{2}} - \Delta x_i)/2\delta x_{i+\frac{1}{2}}$ ,  $\Delta x_i = x_{i+\frac{1}{2}} - x_{i-\frac{1}{2}}$ ,  $\delta x_{i+\frac{1}{2}} = x_{i+1} - x_i$ , and  $\delta x_{i-\frac{1}{2}} = x_i - x_{i-1}$  as shown in figure 1). The other variable that has to be approximated at cell faces is the interface conductivity; the harmonic mean is used for composite materials for its superior handling of abrupt property changes by recognizing that the primary interest is to obtain a good representation of heat flux across interfaces rather than that of the conductivity [PAT 80] :

$$\frac{1}{k} = \frac{1 - f_{i+\frac{1}{2}}}{k_i} + \frac{f_{i+\frac{1}{2}}}{k_{i+1}} \quad (7)$$

In this study, the temporal distributions of temperature is approximated by two-time level schemes [VER 95], such that :

$$\int_t^{t+\Delta t} T dt = [\alpha T - (1 - \alpha)T^0] \Delta T \quad (8)$$

where  $\alpha$  is a weighting factor with the value between 0 and 1.

Three main schemes are considered: explicit, Crank-Nicholson and fully implicit. The first-order accurate explicit method uses temperature gradients of the previous time step  $t$  to calculate the unknown  $T$  at  $t + \Delta t$  such that  $\alpha = 0$ . Hence, the time step size  $\Delta t$  is limited to  $\Delta t < \rho c (\Delta x)^2 / 2k$  for 1D. The second-order accurate Crank-Nicholson scheme uses the average of previous and present temperature gradients to compute the present temperature, by taking  $\alpha = 0.5$  in the above, and hence, has less severe step size limitation than the explicit scheme. The fully implicit scheme, however is unconditionally stable with first-order accuracy at  $\alpha = 1$ .

Taking Figure 1 as reference, the heat equation may be discretized as follows :

$$\rho c \Delta x_i (T_i - T_i^0) = \left[ k_{i+\frac{1}{2}} \frac{\alpha (T_{i+1} - T_i) + (1 - \alpha) (T_{i+1}^0 - T_i^0)}{\delta x_{i+\frac{1}{2}}} - k_{i-\frac{1}{2}} \frac{\alpha (T_i - T_{i-1}) + (1 - \alpha) (T_i^0 - T_{i-1}^0)}{\delta x_{i-\frac{1}{2}}} \right] \Delta t. \quad (9)$$

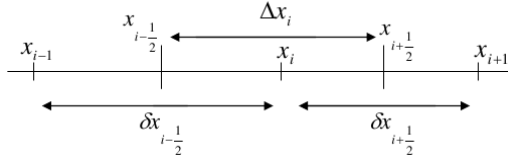


Figure 1: A typical 1D control volume

The convergence and stability of this kind of method could be proven according to the work of [MAG 93].

## 5 Problem reformulation and Latent heat accumulation method

In the basic enthalpy scheme, enthalpy is used as the primary variable and the temperature is calculated from a defined enthalpy-temperature relation :

$$H = \begin{cases} \rho C_s T, & T < T_f \\ \rho C_s T_f + \rho C_l (T - T_f) + \rho L, & T \geq T_f \end{cases} \quad (10)$$

where  $H$  is the enthalpy.

Anticipating the discrete description given in the next section, we suppose now that the physical domain (one dimensional in our case) is divided into a finite number of cells (from now on, the subscript  $i$  refers to a particular volume).

The latent heat accumulation method has been proposed by [PRA 04] and is resumed hereafter. Prior to the first time interval, the accumulated latent heat  $Q_i$  of a control volume  $V_i$  is initialized to zero. At the beginning of each time step, the phase status of each control volume is checked. If the nodal phase is solid

and the nodal temperature  $T_i$  rises higher than the melting temperature  $T_f$ , then control volume becomes saturated and its node is tagged (the cell is called “mushy”). Since an explicit scheme is used, the current temperature may be calculated directly from the previous values. The nodal temperature is then reassigned to the melting temperature and the latent heat increment (the energy used for phase change in the current time step) is calculated from the fictitious sensible heat such that  $\Delta Q_i = \rho C (T_i - T_f) V_i$ , where  $V_i$  is the volume of the cell and  $C$  is calculated as follows:  $C = (1 - \theta)C_l + \theta C_s$ , where the solid fraction  $\theta$  is the percentage of ice present in  $V_i$ .

The  $\Delta Q_i$  quantity is added to the accumulated  $Q_i$  for subsequent time steps until the accumulated latent heat equals the total latent heat  $Q_i^{tot}$  available in the control volume, which is

$$Q_i^{tot} = \int_{V_i} \rho L dv \quad (11)$$

At this stage, the control volume becomes liquid, the tag on the cell is removed and the latent heat increment is no longer calculated.

## 5.1 Basic model with uniform mesh

As a first step, the discretized formula obtained has been applied under the explicit form where the time step must be chosen according to the Cauchy stability criterion:

$$\Delta t < \Delta t_c = \frac{1}{2} \frac{\rho_s C_s \Delta x^2}{k_s}$$

Practically,  $\Delta t$  is always chosen to be equal to  $0.99\Delta t_c$ .

Thermophysical properties used in the calculation are those of the system water/ice. Spatial temperature profiles (Figure 2a; only a quarter of the whole domain is shown) match the analytical solution [PRA 04] very well, but time evolutions (Figure 2b) present some fluctuations, despite the large number of nodes used. These fluctuations are unavoidable: they are due to the finite width of the cell (In fact, the heat flux is blocked during the melting process inside the mushy cell). To overcome this unwanted behavior, the only way is to refine the grid near the interface, leading to the adaptive mesh technique presented below.

## 5.2 Improved model with recursive mesh refinement

It becomes obvious that in order to prevent any non-physical solution, it is advantageous to vary the mesh size according to the position of the interface. A global refinement would be the simplest technique in order to enhance the accuracy of the approximated solution; however, this technique will not be used here due to the high memory required. In general, two types of adaptive techniques are mostly used; the first one is the local refinement method whereby uniform fine grids are added in the regions where the approximated solution lacks adequate accuracy [ASK 87], and the second is the moving mesh technique where nodes are relocated at necessary time steps [MER 00].

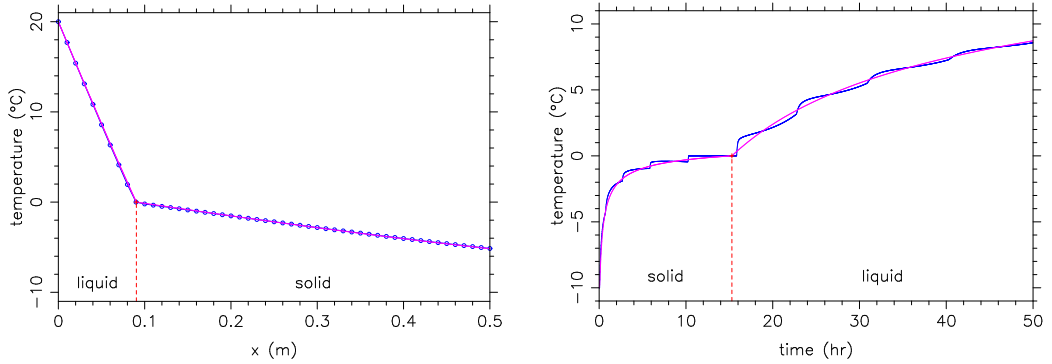
(a) Temperature profile at  $t_{max} = 50 h$ .(b) Temperature history at  $x = 5 cm$ .

Figure 2: Uniform mesh,  $N_{basic} = 200$ ,  $dt = 4.46E + 01 s$ . Analytical (red) and numerical (blue) solutions.

We have chosen a different technique, a classical 'insert/delete nodes' technique for the primal mesh (like Homard [HOM 95], used in FEM but adapted for the finite volume schemes) which has been used with recursive subdivisions, to produce excellent results for the one-dimensional melting problem. The previously described fixed basic uniform mesh is our starting point; then we refine the primal mesh by a number of subdivisions near the phase-change front — at each level of subdivision we add a node at the middle of the two successive nodes (see Figure 3). The melting front is initially located in the first cell and can move anywhere along the discretized domain. When the phase-change front transfers to a new cell, the node added in a previous step is removed and a new node will be added to the new element.

This rolling mesh has the following characteristics:

- the mesh rolls because some nodes are added whereas others are deleted, but only when the mushy cell changes; most of the time the whole mesh remains unchanged;
- only the primal mesh is locally refined; then the dual mesh (*i.e.*, the cell boundary) is updated;
- it is not a moving mesh: during the time evolution all nodes are fixed in position. This fact guarantees a good accuracy due to the small number of needed interpolations (they are needed only when a new node is inserted).

This technique was implemented as a double linked list in Fortran 95. Each item of this list contains information about geometry (cell size) and physical variables (temperature, latent heat accumulation and a tag for the phase state). A number of fixed recursive subdivisions is used depending on the precision needs.



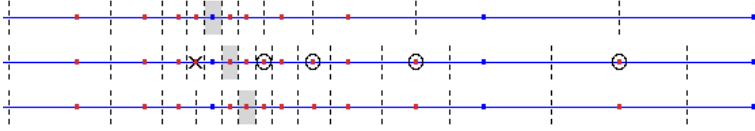


Figure 3: Recursive mesh refinement used to track the phase change front (dot points are nodes whereas dashed lines delimit cells; the mushy cell is colored in grey). Blue points are the basic uniform mesh. Circled points are the new nodes which have been inserted (between steps 1 and 2) to satisfy some constraints on the mesh progressiveness. The crossed point disappears between steps 2 and 3.

### 5.3 Energy conservation during the 'insert/delete nodes' technique

It is well known that the finite volume scheme conserves some extensive quantities. In our case, it is namely the energy used in equation 1, that can be written as follows

$$E = \int \rho C T dx \quad (12)$$

As in our physical model  $\rho$  and  $C$  are constants (in each phase), the integral of temperature must be conserved over the whole mesh during any 'insert/delete' nodes event.

Suppose we must insert a new node or delete an existing one: other temperature values at other nodes should be then modified for  $E$  to be remain unchanged. However, in our refinement technique (described in the previous subsection), we add/delete a node only for the 'mushy' cell (corresponding to a slope discontinuity of the temperature) without any modification. This is because a node is always inserted (or deleted) in a linear temperature behavior as we can see in Figures 4a or 5a.

### 5.4 Results and comments

We have found that the adaptive technique do ameliorates the smoothness (hence the correctness) of the solution. Figures 4 and 5 show numerical results for two different values of the subdivision number. The more we refine the phase-change area, the more we obtain a good accuracy and fewer fluctuations; actually these fluctuations are not eliminated but their amplitude decreases drastically that they seem to vanish (see Figure 7). A good agreement with the analytical solution is shown.

Figure 6a clearly indicates that the local mesh refinement allows the use of a less total number of nodes leading to an economy of memory usage. It also shows errors between the numerical and the analytical solutions, and gives a comparison between the two models used. The relative error is calculated only from the time evolution curve (at  $x = 5 \text{ cm}$ ) via the following Root-Mean-Square formula:

$$Error_{RMS} = \sqrt{\frac{1}{N} \sum_{j=1}^N (T(t_j) - T(t_j)_{exact})^2}.$$

$N$  being the total number of time steps.

Globally, taking into account both precision and computational cost, the proposed scheme is slightly better than the basic one, as shown in Figure 6b. Actually, the performance limitation of our method is due to the use of an explicit scheme which requires us to use a small time step; this should be numerically expensive in the case of large problems. Therefore, this method is poorly suited to multidimensional problem.

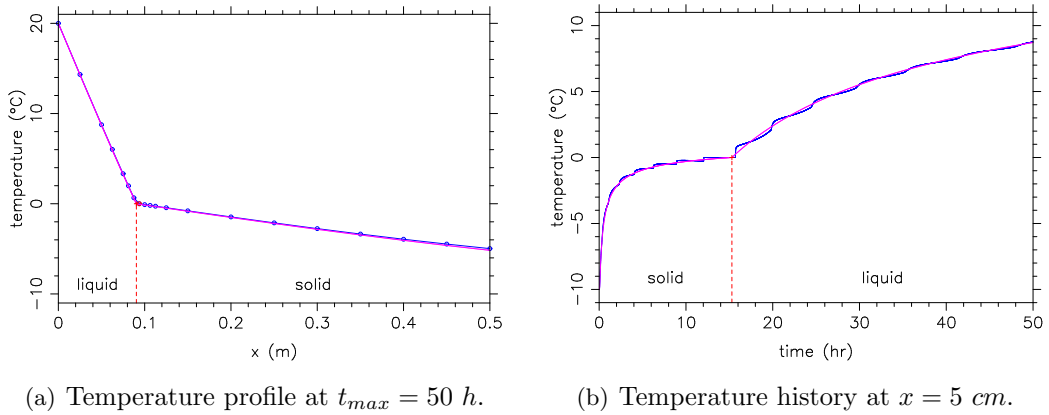


Figure 4: Rolling mesh,  $N_{basic} = 40$ ,  $dt = 1.74E + 01 s$ , number of subdivisions: 3. Analytical (red) and numerical (blue) solutions.

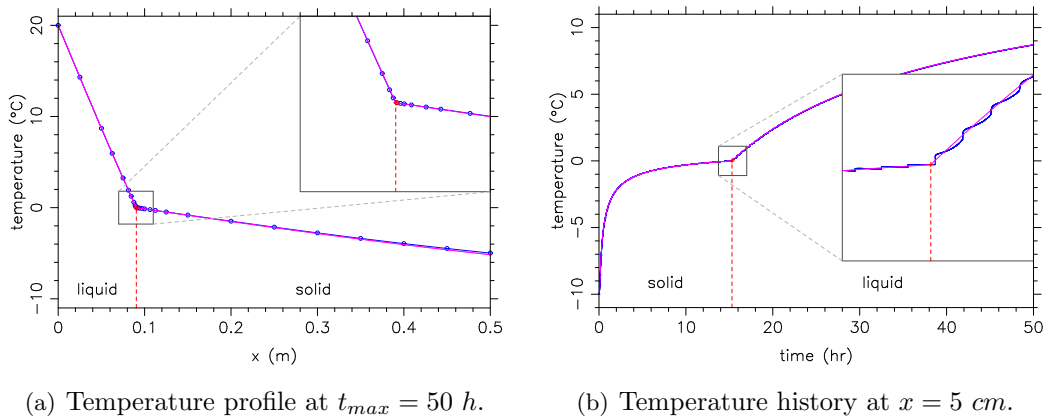
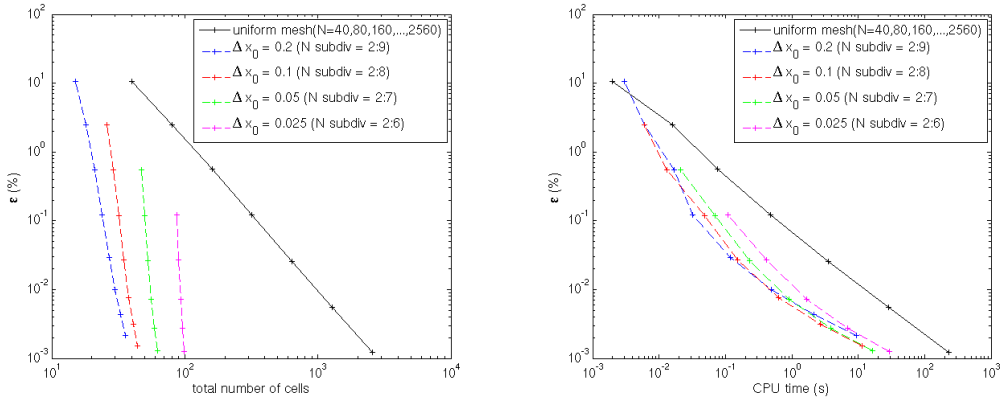


Figure 5: Rolling mesh,  $N_{basic} = 40$ ,  $dt = 2.72E - 01 s$ , number of subdivisions: 6. Analytical (red) and numerical (blue) solutions.

Due to the limitation of the explicit scheme, several implicit ones have been tried (Crank-Nicholson and a fully implicit scheme) to achieve the expected efficiency and computational cost. As previously described, the explicit scheme has a restriction on time step size. Moreover, large time intervals cause the solution to diverge. Crank-Nicholson and fully implicit schemes may employ somewhat larger time steps but because of the structural model accuracy still depends on time step sizes. In addition,



(a) RMS Errors versus the total number of cells. (b) RMS Errors versus the computational time.

Figure 6: explicit scheme.

implicit schemes require more CPU time than the explicit scheme due to the iterative procedures of the solver. Figure 8 shows the limitation of the used approach with the implicit schemes, thus a need of a different approach. However, by using this approach it is difficult to determine the interface position in multidimensional case.

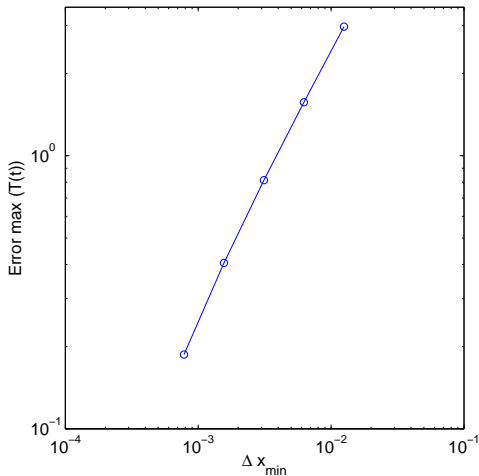


Figure 7: Oscillations amplitude on temperature history.

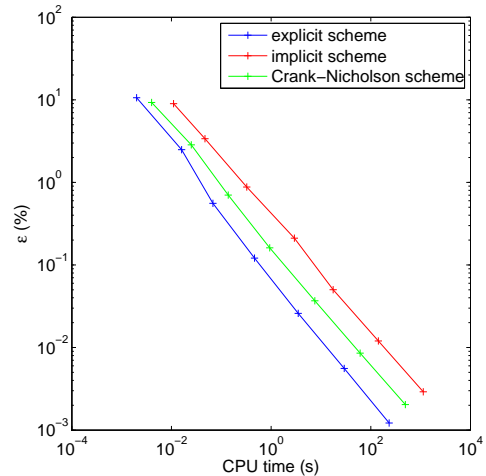


Figure 8: RMS Errors on the temperature history versus the CPU time.

## 6 Apparent heat capacity method

To avoid the tracking of the interface, the apparent heat capacity method will be used. In this method, the latent heat is calculated by integrating the heat capacity over the temperature [BON 73], and the computational domain is considered as one region. As the relationship between heat capacity and temperature in isothermal

problems involves sudden changes, the zero-width phase change interval must be approximated by a narrow range of phase change temperatures. Thus, the size of time steps must be small enough so that this temperature range is not overlooked in the calculation. The equivalent thermodynamic parameters are defined considering the apparent capacity method of [BON 73]. According to this reference, if these properties do not depend on temperature, the equivalent parameters may be obtained taking into consideration that the phase change takes place in a small temperature interval (see Figure 9).

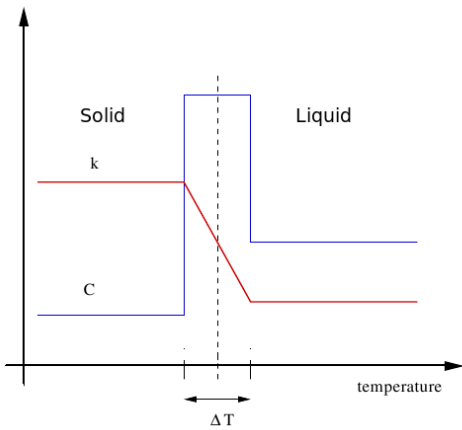


Figure 9: Physical properties given by Bonacina.

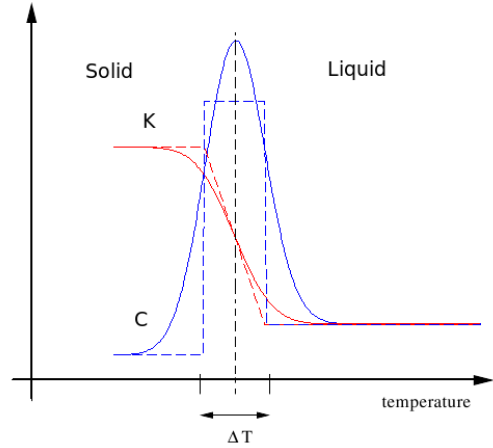


Figure 10: Smoothed physical properties used in this paper.

Then, if this interval is  $\Delta T$ :

$$C = \begin{cases} C_s, & T < T_f - \Delta T \\ \frac{C_l + C_s}{2} + \frac{L}{2\Delta T}, & T_f - \Delta T \leq T \leq T_f + \Delta T \\ C_l, & T > T_f + \Delta T \end{cases} \quad (13)$$

Where  $L$  is the heat of phase change per unit volume [ $J/kg$ ],  $T_f$  is the phase change temperature, and  $\Delta T$  is the temperature semi-interval across  $T_f$ . Similarly a global new thermal conductivity has to be introduced:

$$k = \begin{cases} k_s, & T < T_f - \Delta T \\ k_s + \frac{k_l - k_s}{2\Delta T} [T - (T_f - \Delta T)], & T_f - \Delta T \leq T \leq T_f + \Delta T \\ k_l, & T > T_f + \Delta T \end{cases} \quad (14)$$

Numerical solutions are obtained by using an approach based on a fixed grid and a vertex-centered finite volume discretization. The accuracy and flexibility of the present numerical method are verified by comparing the results with existing analytical solutions. The principal advantages of this approach are that (i) temperature  $T$  is the primary dependent variable which derives directly from the solution, and (ii) the use of this method usually eliminates the fluctuations found by using the LHA approach (see figure 2b). However, the AHC formulation leads to approximated solutions and suffers from a singularity problem for the physical properties

$C$  (specific heat capacity) and  $k$  (conductivity) (see Figure 9). While the explicit form of discretization used in the previous approach is computationally convenient, it has a possible limitation due to the presence of time fluctuations in the solution. Results show the limitation of the LHA method due to the limiting small time step.

The implicit calculation is often worthwhile because the implicit Euler method has no stability limit. However, there is a price to pay for the improved stability of the implicit method, which is solving a system of nonlinear ordinary differential equations. We are going to solve PDEs by using the method of lines, where space and time discretizations are considered separately, leading to semi-discrete systems of ODEs. Fortunately, there is a considerable amount of high quality ODE software available, much of it recently developed. These softwares are used for the integration in  $t$  to achieve stability (or a more sophisticated explicit integrator in  $t$  is used that automatically adjusts  $\Delta t$  to achieve a prescribed accuracy).

The numerical solution can be obtained as the limit of a uniformly convergent sequence of classical solutions to approximating problems, deduced by smoothing the coefficients (13, 14), following few general rules [CIV 87]: The apparent heat capacity formulation allows for a continuous treatment of a system involving phase transfer. If the phase transition takes place instantaneously at a fixed temperature, then a mathematical function such as

$$\phi = U(T - T_f) \quad (15)$$

is representative of the volumetric fraction of the initial phase (ice phase).  $U$  is a step function whose value is zero when  $T < T_f$  and one otherwise. Its derivative, i.e., the variation of the initial phase fraction with temperature, is

$$\frac{d\phi}{dT} = \delta(T - T_f) \quad (16)$$

in which  $\delta(T - T_f)$  is the Dirac delta function whose value is infinity at the transition temperature,  $T_f$ , but zero at all other temperatures. To alleviate this singularity the Dirac delta function can be approximated by the normal distribution function sketched in Figure 11

$$\frac{d\phi}{dT} = (\epsilon\pi^{-1/2})\exp[-\epsilon^2(T - T_f)^2] \quad (17)$$

in which  $\epsilon$  is chosen to be  $\epsilon = 1/\sqrt{2}\Delta T$  and where  $\Delta T$  is one-half of the assumed phase change interval. Consequently, the integral of equation 17 yields the error functions approximations for the initial phase fraction as sketched in Figure 12. With conventional finite volume method, the initial phase fraction derived from equation 17 by integration should be used to avoid the numerical instabilities arising from the jump in the values of the volumetric fraction of initial phase from zero to one. In our approach we assume for simplicity that the phases are isotropic and homogeneous, and the densities of the phases are equal. Accordingly, the smoothed coefficients (see Figure 10) of equations 13 and 14 could be written as:

$$c = c_s + (c_l - c_s)\phi + L\frac{d\phi}{dT} \quad (18)$$

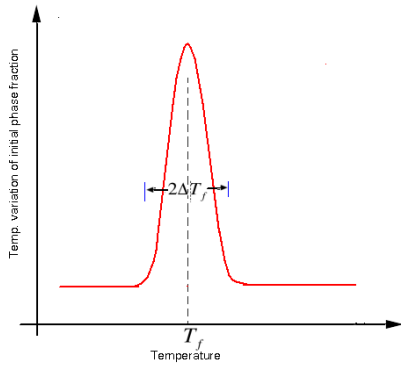


Figure 11: Approximation of the initial phase fraction over a small temperature interval according to the linear functions.

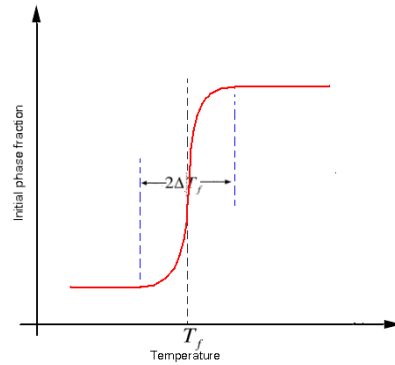


Figure 12: Approximation of the initial phase fraction over a small temperature interval according to the error functions.

and

$$k = k_s + (k_l - k_s)\phi \quad (19)$$

## 6.1 Global resolution using the Method of lines

The problem to be solved may be written in vectorial form with adequate initial and boundary conditions:

$$\frac{\partial T}{\partial t} = f(t, x, T) \quad (20)$$

The user is typically required to write a simple routine which evaluates the function  $f$  when the arguments  $t$ ,  $x$ ,  $T$ ,  $\partial T/\partial x$ , ... are provided. Other equally simple subprograms would be required to specify appropriate boundary and/or initial conditions.

With generalization in mind, a numerical strategy inspired by the treatment of ordinary differential equations (ODE) associated to space discretization using the method of lines is applied [HUN 03]. It allows:

- a global treatment of the system without discrimination between the variables.
- a treatment of the physical model in its original form, as it was written, without preliminary manipulations.
- the use of sophisticated methods which have been developed for initial value differential equations.
- the possibility, for further works, to use the developments involved in ODE systems (parameter estimation, sensitivity analysis...)

The main failures of the method are the large size of the resulting ODE system obtained after discretization (this problem can be reduced by using an adequate numerical conditioning of the system) and the rigidity of the fixed grid discretization

scheme which is not really a problem in our case and could be solved by using an adaptive mesh.

The numerical method of lines consists in discretizing the spatial variable into  $N$  discretization points. Each state variable  $T$  is transformed into  $N$  variables corresponding to its value at each discretization point. The spatial derivatives are approximated by using a finite volume formula on 3 points where the best results for accuracy and computation time efficiency were obtained. We are solving PDEs, where space and time discretizations are considered separately this lead to a semi-discrete system of ODEs, which can be written as:

$$T' = A(T)T \quad (21)$$

The Jacobian matrix  $A(T)$  is computed explicitly (its tridiagonal structure is due to the 1-D laplacian discretization). The ODE solver has been modified in such a way that the Jacobian matrix  $A(T)$  could be coded by hand in sparse format. The numerical calculation is performed with `ddebdf` routine of the SLATEC Fortran library [BRE 89]. This is designed to simulate systems of coupled non-linear and time dependent partial differential equations. It is used for the time integration to achieve stability and a prescribed accuracy by adjusting automatically the time step in the Backward Differentiation Formula (BDF). The BDF method is well adapted to our problem which becomes more and more stiff as  $\Delta T$  decreases (see Figure 16).

## 6.2 Results and comments

The accuracy and flexibility of the present numerical method are verified by comparing the results with existing analytical solutions [BEJ 03]. Figures 13a and 14a present the temperature profile for different values of  $\Delta T$ , with spatial discretization  $N = 320$ . Figures 13b and 14b show the related histories of temperature at  $x = 5 \text{ cm}$ . It is evident that the accuracy of the AHC method is sensitive to the magnitude of  $\Delta T$  that is arbitrarily selected to approximate the Dirac delta function or to distribute the latent heat.

We introduce a quality factor for each solution which combines accuracy and smoothness according to the relation:

$$\text{Quality factor} = \text{Error}_{\text{RMS}}(T) + 0.025 \text{Error}_{\text{RMS}}(T') \quad (22)$$

Since the apparent heat capacity method approaches the exact analytical solution as the assumed temperature interval approaches zero, it is shown that the apparent heat capacity method can produce both smooth and accurate solutions.

It appears from these numerical solutions that the results obtained by approximating the phase change at a fixed temperature by a gradual change over a small temperature interval should be acceptable if

$$\frac{2\Delta T}{|T_i - T_f|} < 0.1 \quad (23)$$

where  $T_i$  is the temperature of the control volume  $V_i$ .

In Figure 15, we can see that there is a minimum for the quality factor corresponding to an assumed value of  $\Delta T$ . This minimum has been drawn as  $\Delta x$  in Figure 17.

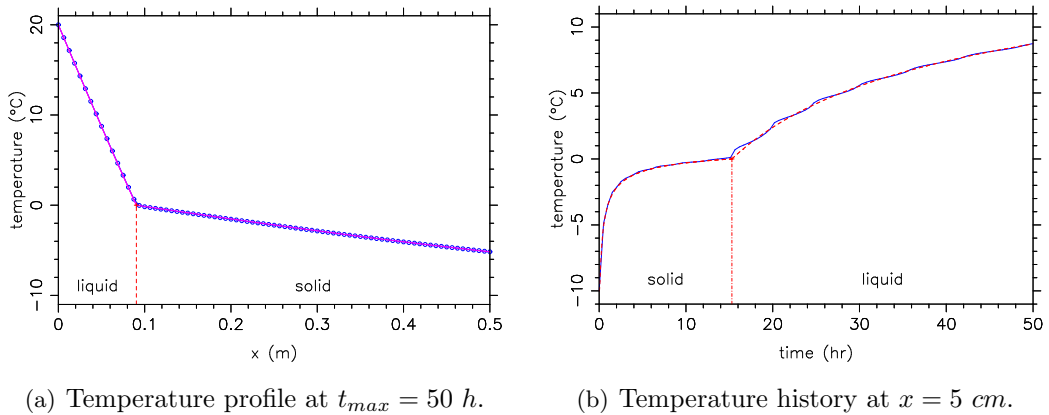


Figure 13:  $N_{basic} = 300$ .  $\Delta T = 0.1^\circ C$ . Analytical (red) and numerical (blue) solutions.

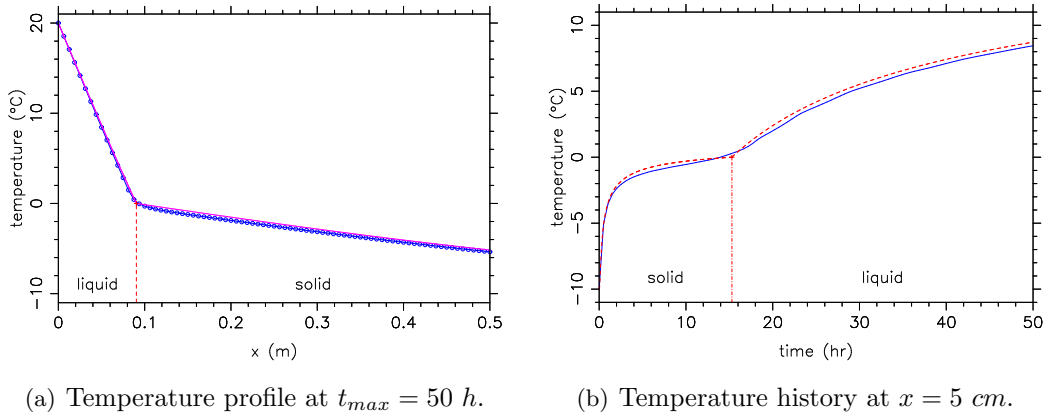


Figure 14:  $N_{basic} = 300$ .  $\Delta T = 0.5^\circ C$ . Analytical (red) and numerical (blue) solutions.

## 7 Comparison between the two methods

Practically in phase change situations, more than one phase change interface may occur or the interfaces may disappear entirely. Furthermore, the phase change usually happens in a non-isothermal temperature range. In such cases, tracking the solid-liquid interface may be difficult or even impossible. Calculation-wise, it is advantageous that the problem is reformulated in such a way that the Stefan condition is implicitly bounded up in a new form of the equations and that the equations are applied over the whole fixed domain. This can be done by determining what is known as the enthalpy function  $H(T)$  and by using the AHC approach. The LHA method has the great advantage which is the accuracy of the solution, but this method suffers from fluctuations which are covered by a local refinement of the discretization near the interface. The major problem of this method is that in numerical terms, we are using an explicit parabolic scheme, and this is very penalizing when used with adaptive refinement. For the moment, the problem is solved in 1-D.



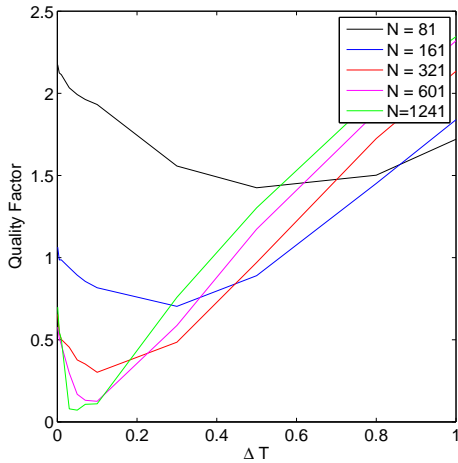


Figure 15: Quality factor versus the magnitude of the assumed temperature interval for different number of nodes.

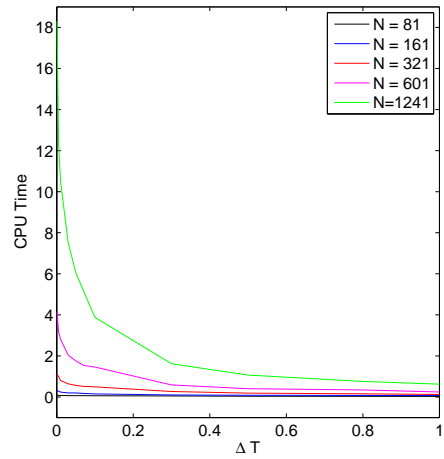


Figure 16: CPU-Time versus the magnitude of the assumed temperature interval for different number of nodes.

In 2 and 3 dimensions we can expect major difficulties in terms of implementation (in particular, the determination of the interface position) and cost (due to the use of an explicit scheme).

With the AHC approach, it is also possible to describe the non-isothermal phase change. This proposed model is solved by using the method of lines with which the fluctuations found in the LHA approach can be avoided by choosing an appropriate value of  $\Delta T$ . Otherwise, it is evident that the error and the order of precision is more pronounced due to approximating the singularity (Dirac delta function) by a gradual change over a small temperature interval. Another observation is that the effect of distributing the latent heat over a temperature interval diminishes as the ratio of temperature interval to the overall temperature variation of the system becomes smaller. It is evident that the AHC method can produce accurate and smooth solutions. Perhaps the biggest criticism to be lodged against this method is that in its standard implementation it requires too much storage for each of the unknown quantities being computed. This would be quite excessive to the person interested in solving a 3-D time dependent problem who is required to use only several locations per point in the problem. However, the presented approach for solving non-linear heat conduction problems is very relevant and we can say that we are presenting one of the most efficient algorithms which takes into account the simplicity of implementation and the desired accuracy. Examples have demonstrated the accuracy reached. Figure 18, illustrates the temperature histories at  $x = 5 \text{ cm}$  obtained by using the two presented approaches.

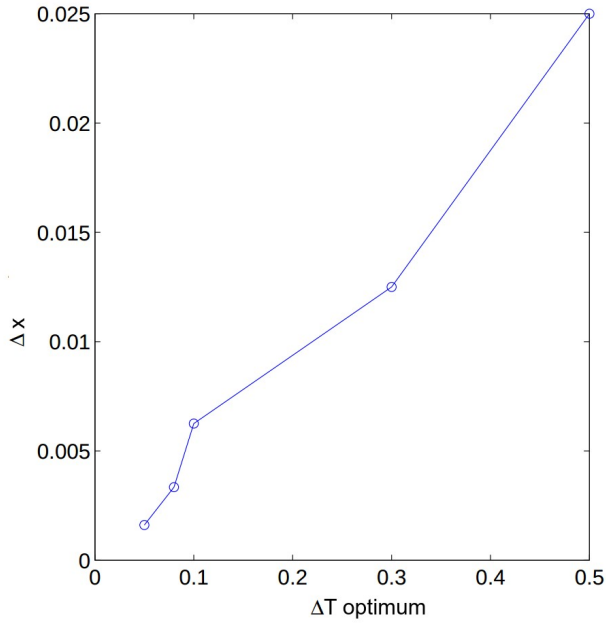


Figure 17:  $\Delta T$  optimum versus the  $\Delta x$

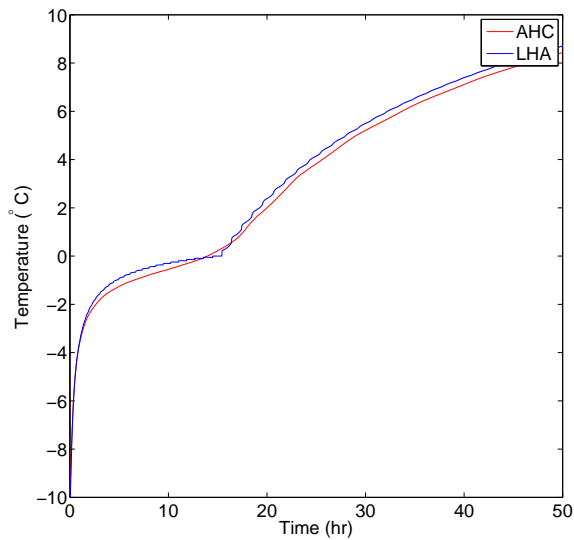


Figure 18: Comparison between the temperature history at  $x = 5$  cm obtained by the LHA (Number of subdivision= 5 and  $N_{basic} = 80$ ) and the one obtained by the AHC ( $\Delta T = 0.5^\circ C$  and  $N_{basic} = 320$ )

## 8 Acknowledgement

This work has been done in the frame of ARPHYMAT<sup>1</sup> collaboration, with a financial support from the “Ministère de l’Éducation Nationale et de la Recherche, France”.

## 9 Bibliography

- [ASK 87] ASKAR H. G., (1987), “The front-tracking scheme for the one-dimensional freezing problem”, *Int. J. of Num. Methods in Engng*, Vol. 24, N. 5, pp 859-869.
- [BEJ 03] BEJAN A. and KRAUS A. D.,(2003), *Heat Transfer Handbook*, Wiley.
- [BON 73] BONACINA C., COMINI G., FASANO A. and PRIMICERIO M., (1973), “Numerical solution of phase-change problems”, *Int. J. Heat Mass Transfer*, Vol. 16, N. 10, pp 1825-1832.
- [BRE 89] BRENNAN K. E., CAMPBELL S. L. and PETZOLD L. R., (1989), *Numerical Solution of Initial-Value Problems in Differential-Algebraic Equations*, Elsevier.  
<http://www.netlib.org/slatec/index.html>
- [CAN 67] CANNON J. R. and HILL C. D., (1967), “Existence, uniqueness, stability and monotone dependence in a Stefan problem for the heat equation”, *J. Math. Mech.*, Vol. 17, N. 1, pp 1-19.
- [CAR 59] CARSLAW H. S. and JAEGER J. C., (1959), *Conduction of Heat in Solids*, Oxford Clarendon Press.
- [CIV 87] CIVAN F. and SLIEPCEVICH C. M., (1987), “Limitation in the Apparent heat capacity formulation for heat transfer with phase change”, *Proc. Okla. Acad. Sci.*, Vol. 67, 1987, pp 83-88.
- [GRA 89] GRANDI G. M. and FERRERI J. C., (1989), “On the solution of heat conduction problems involving heat sources via boundary-fitted grids”, *Comm. in Appl. Num. Methods*, Vol. 5, N. 1, pp 1-6.
- [GUI 74] COMINI G., DEL GUIDICE S., LEWIS R. W. and ZIENKIEWICZ O. C., (1974), “Finite Element Solution of Non-linear Heat Conduction Problems with Special Reference to Phase Change”, *Int. J. Num. Methods in Engng*, Vol. 8, N. 3, pp 613-624.
- [HOM 95] NICOLAS N., ARNOUX-GUISSE F. and BONNIN O., (1995), “Adaptive meshing for 3D Finite Element Software”, in *IX Int. Conf. on Finite Elements in Fluids*, Venice, Italy.  
<https://www.code-aster.org/V2/outils/homard/index.en.html>
- [HUN 03] HUNSDORFER W. and VERWER J., (2003), *Numerical Solution of Time-Dependent Advection-Diffusion-Reaction Equations*, Springer.

<sup>1</sup>ARPHYMAT (ARchæology, PHYsics and MAThematics) is an interdisciplinary project involving three laboratories (the two laboratories mentioned in the first page and the Institute of Physics of Rennes, UMR 6251).

- [JAV 06] JAVIERRE E., VUIK C., VERMOLEN F. J. and VAN DER ZWAAG S., (2006), “A comparison of numerical models for one-dimensional Stefan problems”, *J. of Comput. and Applied Math.*, Vol. 192, N. 2, pp 445-459.
- [KIM 90] KIM C.-J. and KAVIANY M., (1990), “A numerical method for phase-change problems”, *Int. J. Heat Mass Transfer*, Vol. 33, N. 12, pp 2721-2734.
- [KU 90] KU J. Y. and CHAN S. H., (1990), “A generalized Laplace transform technique for phase-change problems”, *J. Heat Transfer*, Vol. 112, N. 2, pp 495-497.
- [LAM 04] LAMBERG P., LEHLINIEMI R. and HENELL A. M., (2004), “Numerical and experimental investigation of melting and freezing processes in phase change material storage”, *Int. J. of Thermal Sciences*, Vol. 43, N. 3, pp 277-287.
- [LUI 68] LUIKOV A. V., (1968), *Analytical heat Diffusion Theory*, Academic Press.
- [MAG 93] MAGENES E. and VERDI C., (1993), “Time discretization schemes for the Stefan problem in a concentrated capacity”, *Meccanica*, Vol. 28, N. 2, pp 121-128.
- [MÉR 00] MÉRIAUX M. and PIPERNO S., (2000), “Méthodes de Volumes Finis en maillages variables pour des équations hyperboliques en une dimension”, Rapport de recherche N. 4042, Inria.
- [MUE 65] MUEHLBAUER J. C. and SUNDERLAND J. E., (1965), “Heat conduction with freezing or melting”, *Appl. Mech. Rev.*, Vol. 18, pp 951-959.
- [MUH 08] MUHIEDDINE M. and CANOT É., (2008), “Recursive mesh refinement for vertex centered FVM applied to a 1-D phase-change problem”, in *Proceedings of the FVCA5 Conference*, Aussois, France, Hermès-Penton, pp 601-608.  
<https://perso.univ-rennes1.fr/edouard.canot/zohour/>
- [PAT 80] PATANKAR S., (1980), *Numerical Heat Transfer and Fluid Flow*, Hemisphere Publishing Corp.
- [PAW 85] PAWLOW I., (1985), “Numerical solution of a multidimensional two-phase Stefan problem”, *Num. Funct. Anal. and Optimiz.*, Vol. 8, pp 55-82.
- [PRA 04] PRAPAINOP R. and MANEERATANA K., (2004), “Simulation of ice formation by the Finite Volume method”, *Songklanakarinn J. Sci. Technol*, Vol. 26, N. 1, pp 55-70.
- [SAV 03] SAVOVIC S. and CALDWELL J., (2003), “Finite difference solution of one-dimensional Stefan problem with periodic boundary conditions”, *Int. J. of Heat and Mass Transfer*, Vol. 46, N. 15, pp 2911-2916.
- [VER 95] VERSTEEG H. K. and MALALASEKERA W., (1995), *An introduction to CFD: the Finite Volume Method*, Longman Scientific & Technical.
- [VOL 87] VOLLER V. R., CROSS M. and MARKAIOS N. C., (1987), “An enthalpy method for Convection/Diffusion phase change”, *Int. J. Num. Methods in Engng*, Vol. 24, pp 271-284.
- [WAN 00] WANG X. F., LIANG H. S., LI Q. and DENG Y. L., (2000), “Tracking of a moving interface during a 2D melting or solidification process from measurements on the solid part only”, in *Proceedings of the 3<sup>rd</sup> World Congress on Intelligent Control and Automation*, Hefei, P. R. China, pp 2240-2243.